Supplementary Information

Tris(Imidazolyl) Dicopper(I) Complex and its Reactivity to Exert Catalytic Oxidation of Sterically Hindered Phenol Substrates via a $[Cu_2O]^{2+}$ Core

By

*Chih-Yu Chen and Ming-Li Tsai**

Department of Chemistry, National Sun Yat-sen University, Kaohsiung 80424, Taiwan

*Corresponding author. E-mail: mltsai@mail.nsysu.edu.tw

Contents

Fig. S5 The bonding interactions between Cu ion and BIMETA in **1** analyzed by ETS-NOCV methods. The key SFOs and the associated deformation densities for (a) charge transfer from ligand 2p to Cu 4s orbitals; (b) charge transfer from ligand 2p to Cu $4p_x/4p_y$ orbitals. Note that the blue and red color shown in the deformation densities represents the increase and decrease of the electron densities, respectively.

Fig. S6 $CO_{(g)}$ and $O_{2(g)}$ binding of complex **1** in CH_3CN solution characterized by UV-vis absorption spectroscopy

Fig. S7 The UV-vis absorption spectra of PhIO-titration reactions into the CH_3CN solution of complex **1** at -40 °C. Each UV-vis absorption spectrum was measured after addition of 0.1/0.2 equiv of PhIO dissolved CH_3CN solution. The increase of a characteristic absorption band of complex $\mathbf{1^{ox}}$ at 640 nm was monitored upon addition of different equiv PhIO.

Fig. S8 The IR spectra of $^{16}O_2$-generated (black) and $^{18}O_2$-generated (red) complex $\mathbf{1^{ox}}$

Fig. S9 The full-range ESI mass spectra of (a) $^{16}O_2$-generated $\mathbf{1^{ox}}$**;** (b) $^{18}O_2$-generated $\mathbf{1^{ox}}$, and the isotope distribution pattern of $^{18}O_2$-generated $\mathbf{1^{ox}}$.

Fig. S10 Typical IR signature and structure of dicopper(II)-bis-μ-hydroxo in relevant papers.

Fig. S11 The isotope distribution pattern of $^{16}O_2$-generated $\mathbf{1^{ox}}$ measured by ESI-MS and its simulated spectrum including dicopper(II)-bis-μ-hydroxo.

Fig. S12 The ^1H NMR spectrum resulting from the stochiometric reaction between TBBP and complex $\mathbf{1^{ox}}$

Fig. S13 The ^1H NMR spectrum resulting from the stochiometric reaction between DTBP and complex $\mathbf{1^{ox}}$

Fig. S14 The proposed mechanism for the formation of TBOBF from the reaction of DTBP and complex $\mathbf{1^{ox}}$

Fig. S15 The ^1H NMR spectra of catalytic ytic oxidation of DTBP with different mol% loading of complex $\mathbf{1^{ox}}$ (2 ~ 10 mol%)

Fig. S16 The ^1H NMR spectra of time-course analysis (10 min ~ 240 min) of product distributions (10 mol% loading of catalyst $\mathbf{1^{ox}}$)

Scheme S1 The energy profile associated with reaction of two equivalents of $[Cu^I(\mu\text{-bimeta})_3Cu^I]^{2+}$ with O_2 generating the corresponding $2[Cu^{II}(\mu\text{-oxo})(\mu\text{-bimeta})_3Cu^{II}]^{2+}$

Table S1 Selected bond distances (Å) and bond angles (°) of **1** and the corresponding DFT structure

Table S2 Summary of crystallographic data, intensity collection and structure refinement parameters for complexes **1**.

(a)

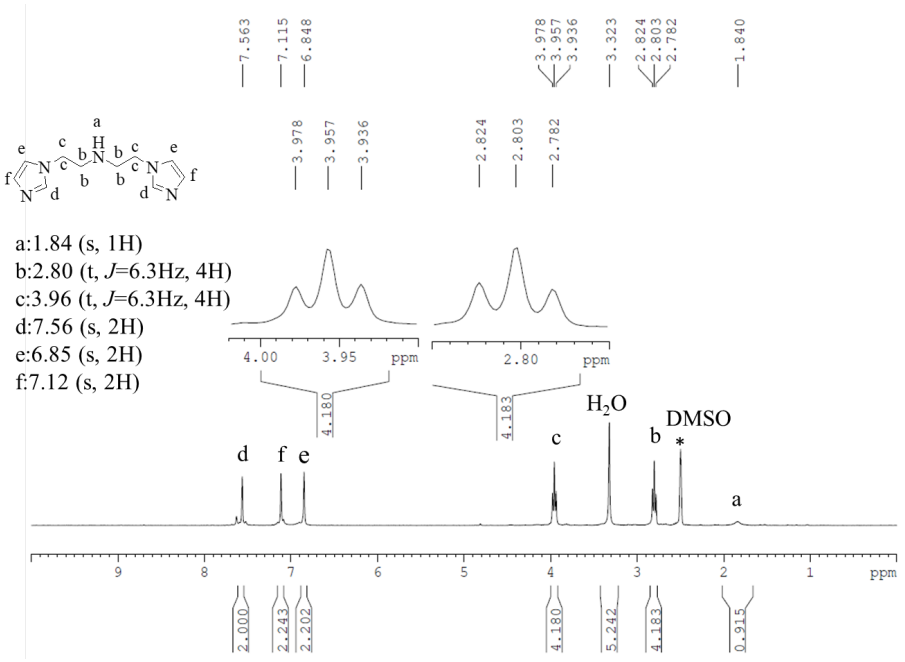
a:1.84 (s, 1H)
b:2.80 (t, J=6.3Hz, 4H)
c:3.96 (t, J=6.3Hz, 4H)
d:7.56 (s, 2H)
e:6.85 (s, 2H)
f:7.12 (s, 2H)
H2O
DMSO
ppm

(b)

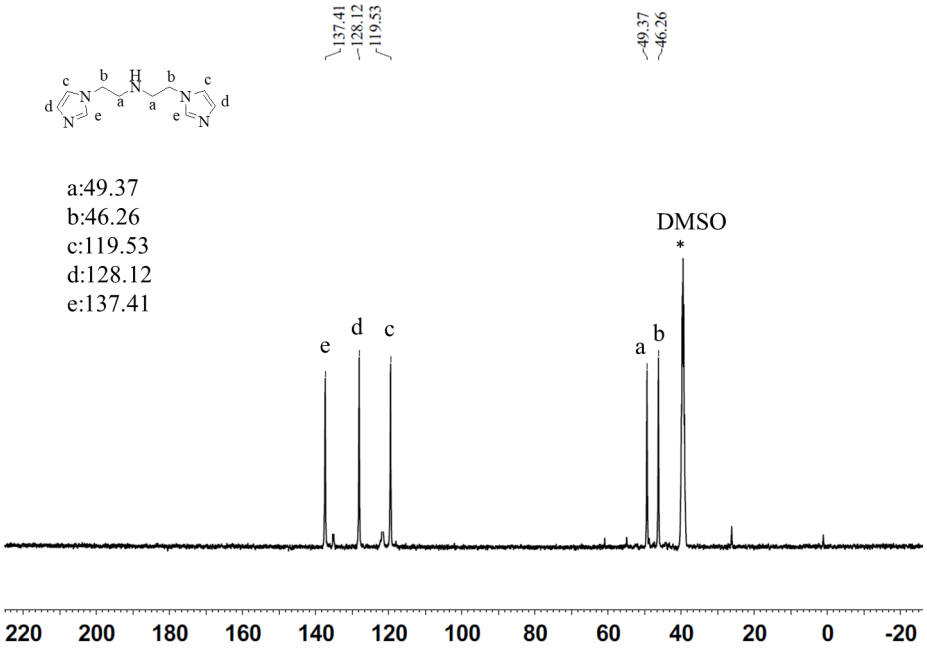
a:49.37
b:46.26
c:119.53
d:128.12
e:137.41
DMSO
ppm

(c)

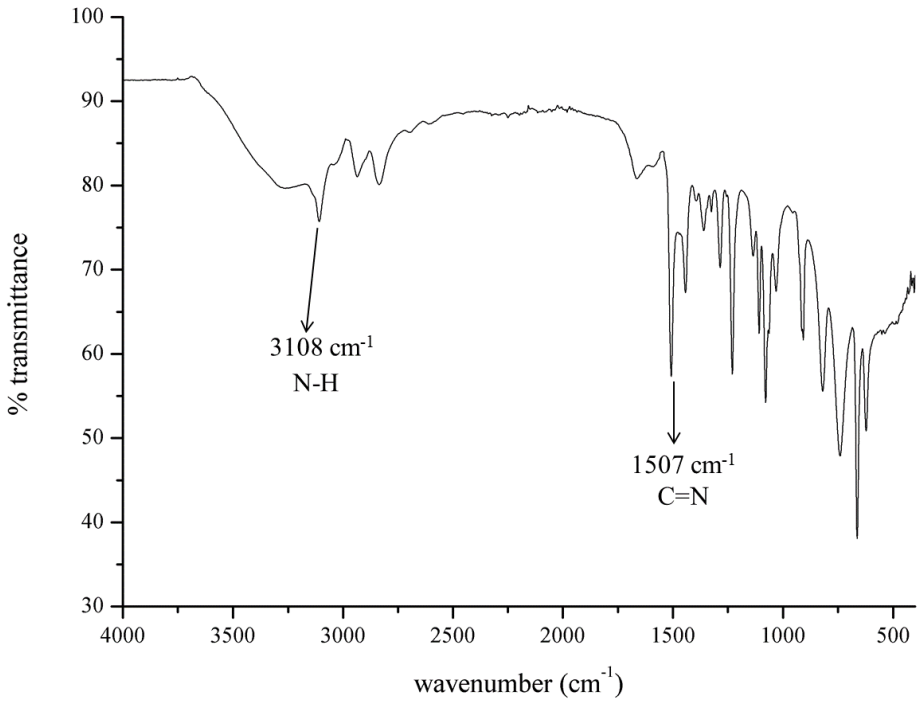

(d)

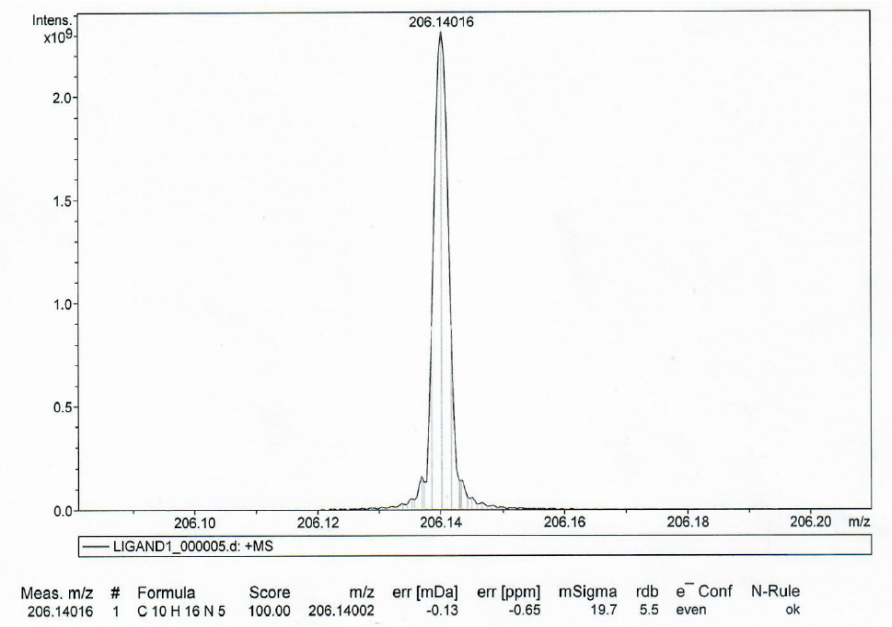

Fig. S1 The (a) ^{1}H NMR and (b) ^{13}C NMR spectra (c) IR (d) high-resolution FT-Mass of bimeta ligand and the assignments of the corresponding peaks/signals.

(a)

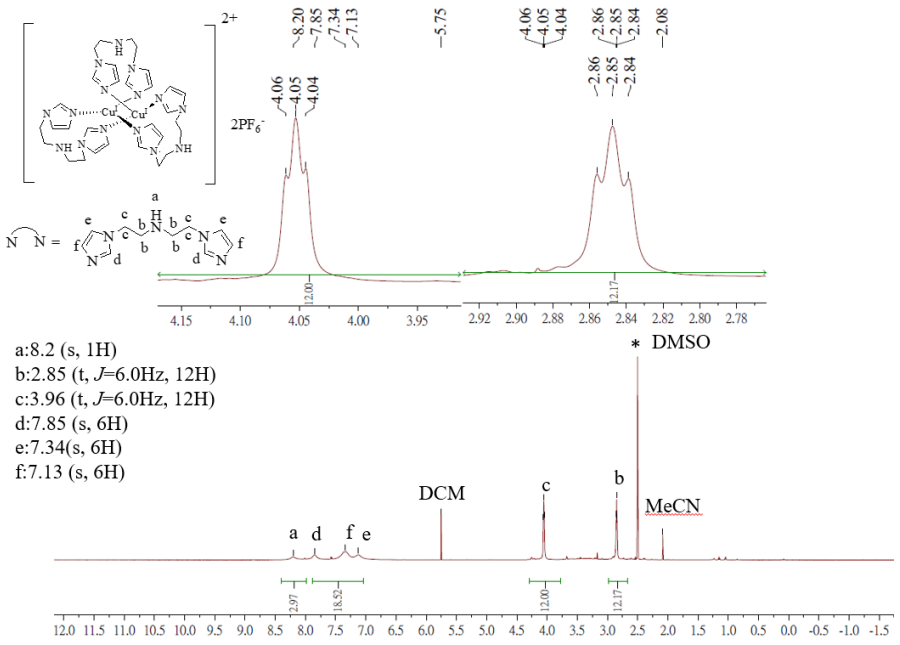

(b)

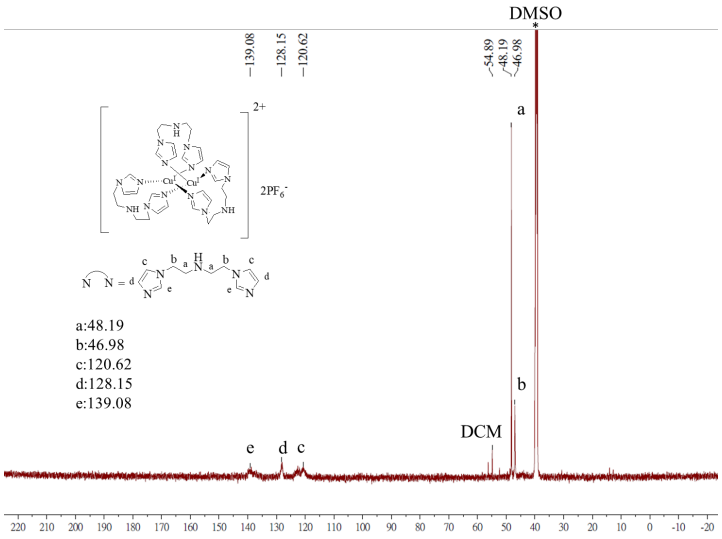

Fig. S2 The (a) ^{1}H NMR and (b) ^{13}C NMR spectra of complex **1** and the assignments of the corresponding peaks/signals.

(a)

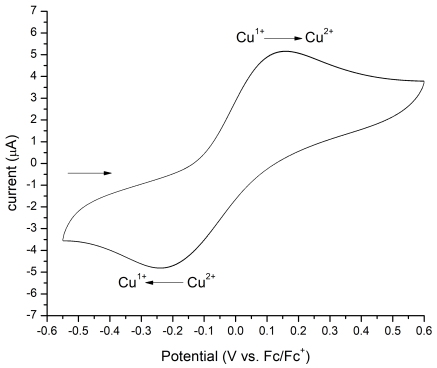

(b)

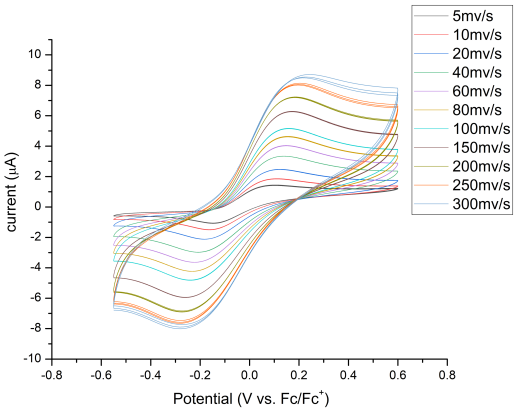

(c)

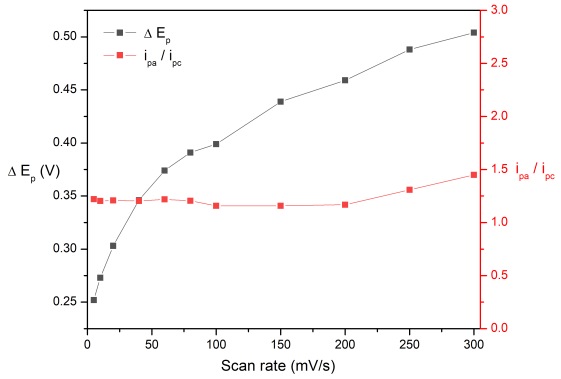

Fig. S3 (a) The cyclic voltammograms of complex **1** measured in CH_3CN with 0.1 M $[^nBu_4N][PF_6]$ and a glass carbon serving as a supporting electrolyte and working electrode, respectively, at a scan rate of 100 mV. (b) the variable-scan-rate CV (5~ 300 mV) measurements of complex **1** in in CH_3CN with 0.1 M $[^nBu_4N][PF_6]$. (c) The ΔE_p vs. scan rate and i_{pa}/i_{pc} vs. scan rate plots

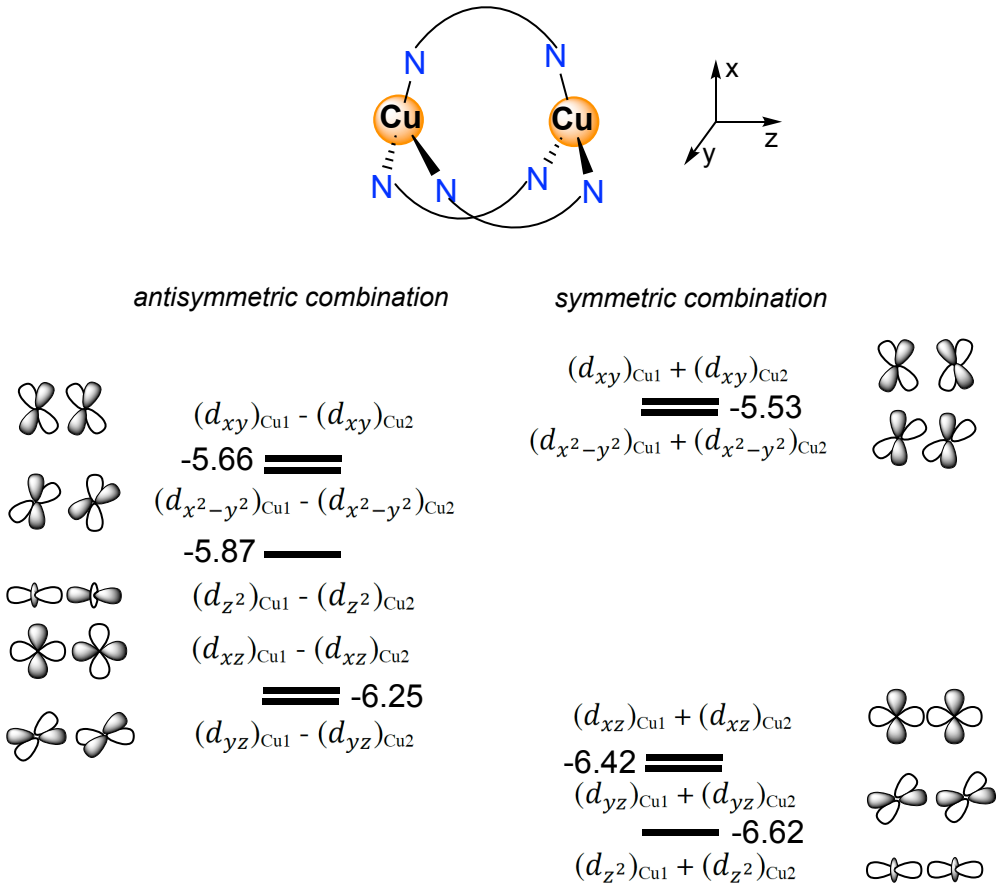

Fig. S4 The schematic representation of d-orbital splitting pattern of complex **1** derived from DFT calculations. Note that the energy of each d orbital pair is shown in eV.

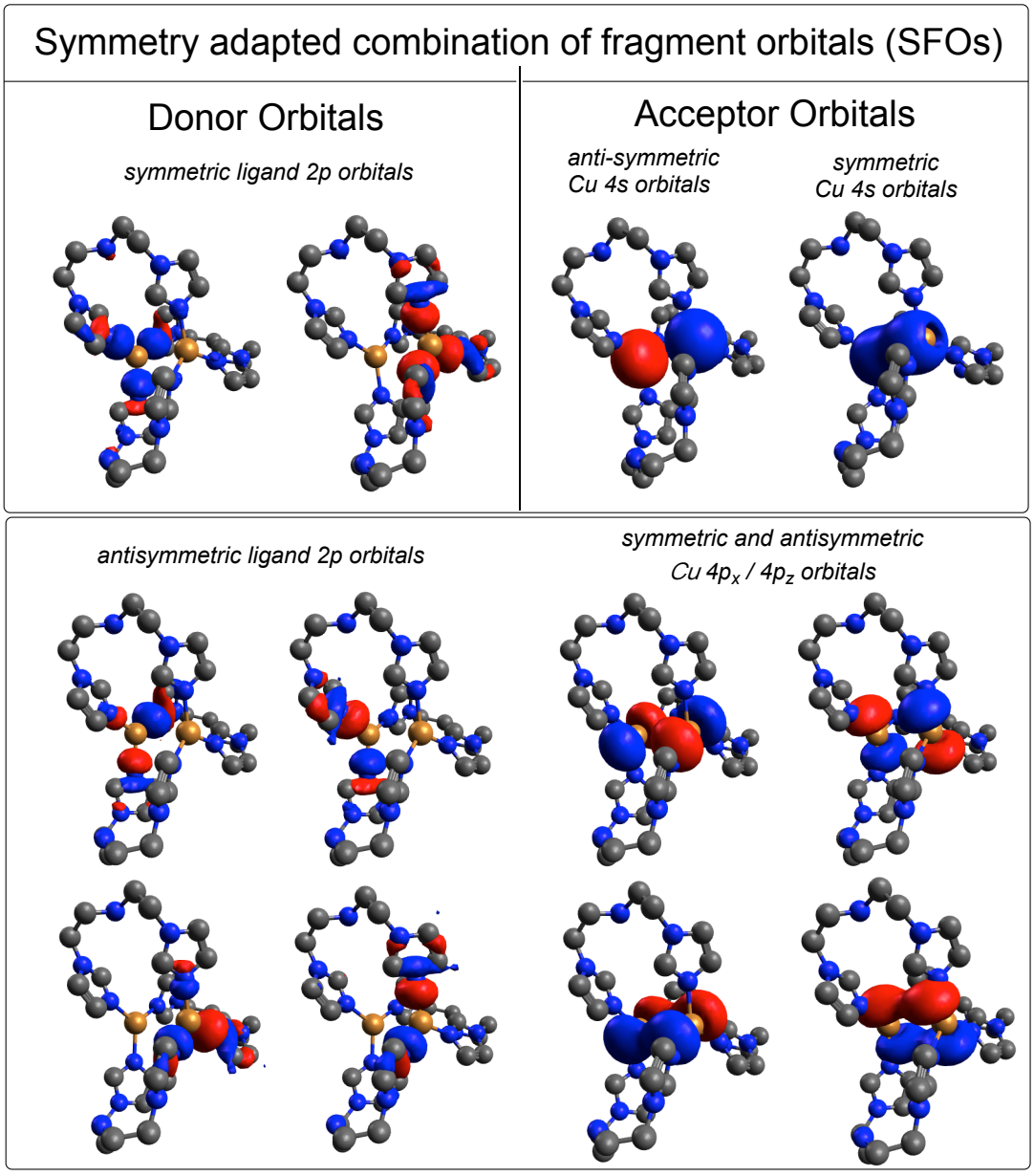

Fig. S5 The bonding interactions between Cu ion and BIMETA in **1** analyzed by ETS-NOCV methods. The key SFOs and the associated deformation densities for (a) charge transfer from ligand 2p to Cu 4s orbitals; (b) charge transfer from ligand 2p to Cu $4p_x/4p_y$ orbitals. Note that the blue and red color shown in the deformation densities represents the increase and decrease of the electron densities, respectively.

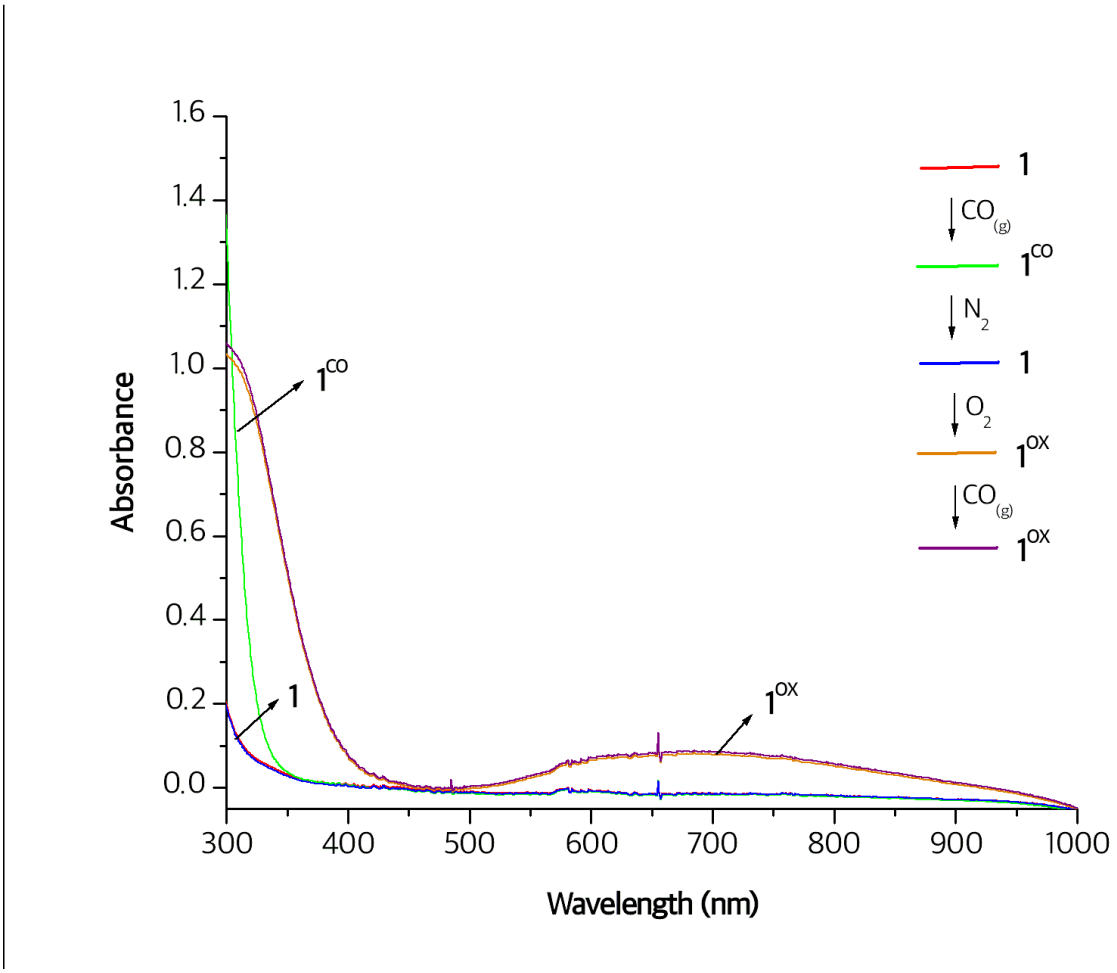

Fig. S6 $CO_{(g)}$ and $O_{2(g)}$ binding of complex **1** in CH_3CN solution characterized by UV-vis absorption spectroscopy

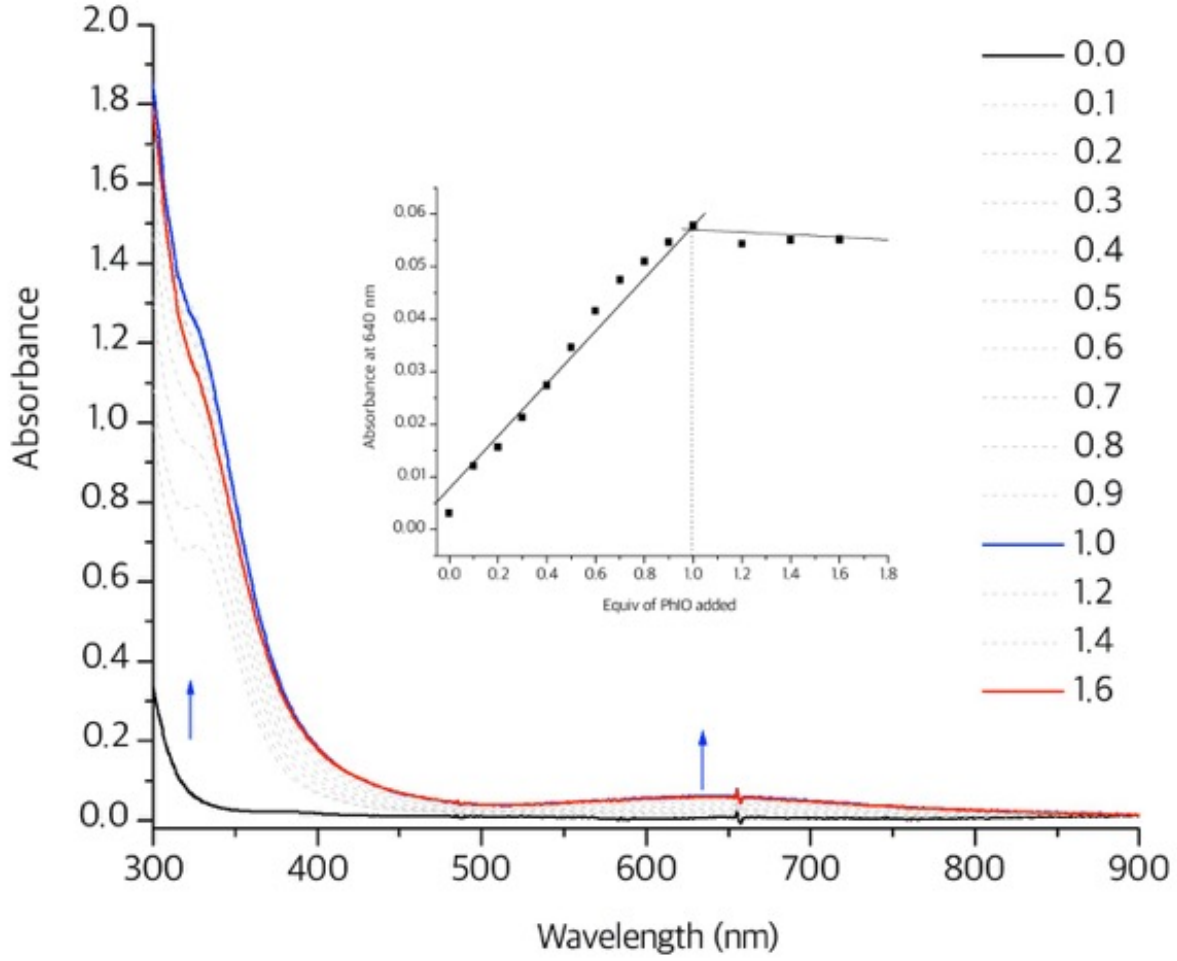

Fig. S7 The UV-vis absorption spectra of PhIO-titration reactions into the CH_3CN solution of complex **1** at -40 °C. Each UV-vis absorption spectrum was measured after addition of 0.1/0.2 equiv of PhIO dissolved CH_3CN solution. The increase of a characteristic absorption band of complex $\mathbf{1}^{ox}$ at 640 nm was monitored upon addition of different equiv PhIO.

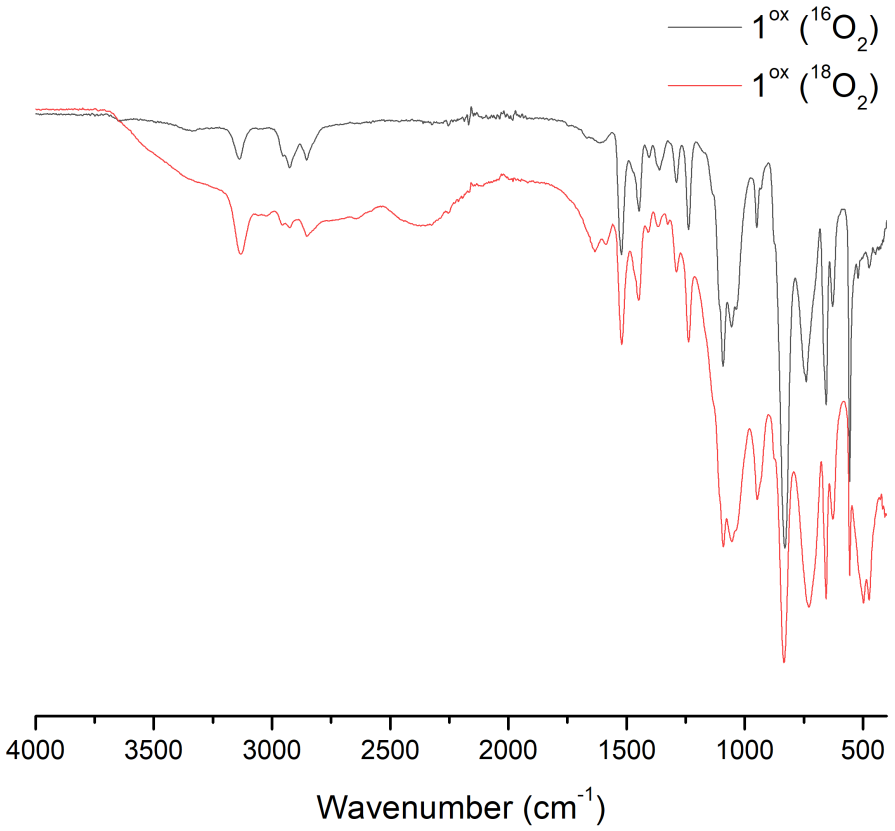

Fig. S8 The IR spectra of $^{16}O_2$-generated (black) and $^{18}O_2$-generated (red) complex **1**^{ox}

(a)

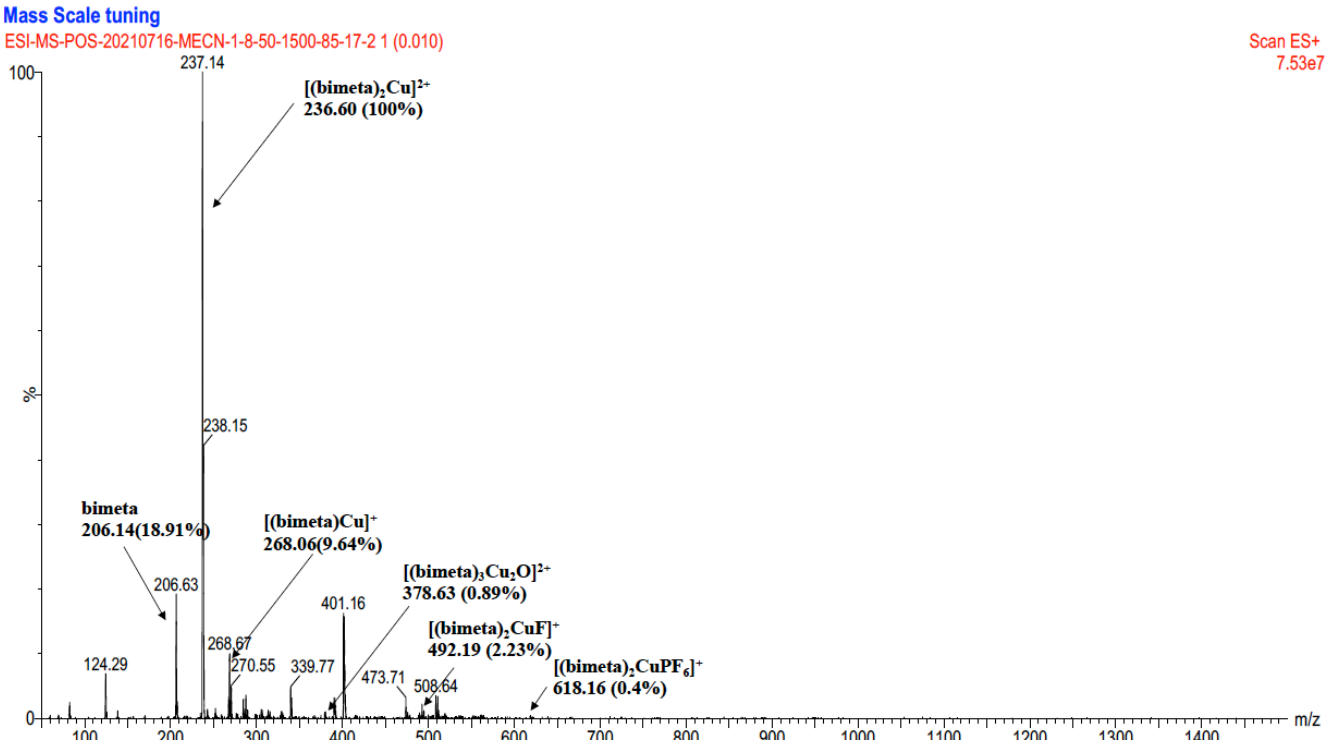
Mass Scale tuning
ESI-MS-POS-20210716-MECN-1-8-50-1500-85-17-2 1 (0.010)
Scan ES+
7.53e7
100
%
0
237.14
[(bimeta)2Cu]2+
236.60 (100%)
238.15
bimeta
206.14(18.91%)
206.63
[(bimeta)Cu]+
268.06(9.64%)
268.67
270.55
[(bimeta)3Cu2O]2+
378.63 (0.89%)
401.16
[(bimeta)2CuF]+
492.19 (2.23%)
124.29
339.77
473.71
508.64
[(bimeta)2CuPF6]+
618.16 (0.4%)
100
200
300
400
500
600
700
800
900
1000
1100
1200
1300
1400
m/z

(b)

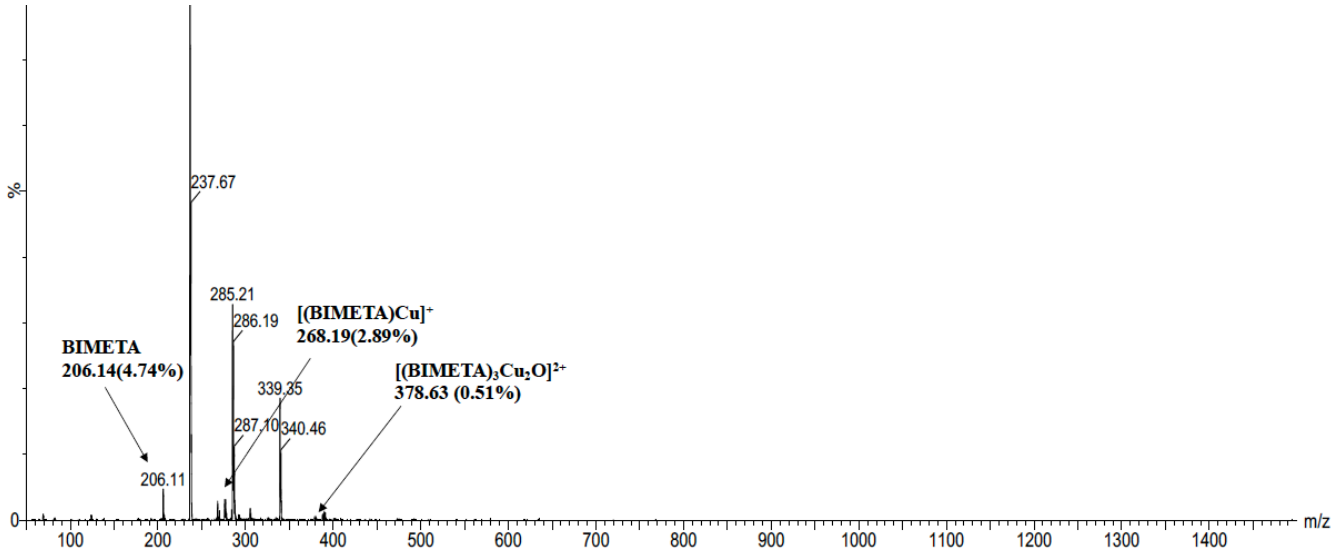
%
0
237.67
285.21
286.19
[(BIMETA)Cu]+
268.19(2.89%)
BIMETA
206.14(4.74%)
[(BIMETA)3Cu2O]2+
378.63 (0.51%)
339.35
287.10
340.46
206.11
100
200
300
400
500
600
700
800
900
1000
1100
1200
1300
1400
m/z

(c)

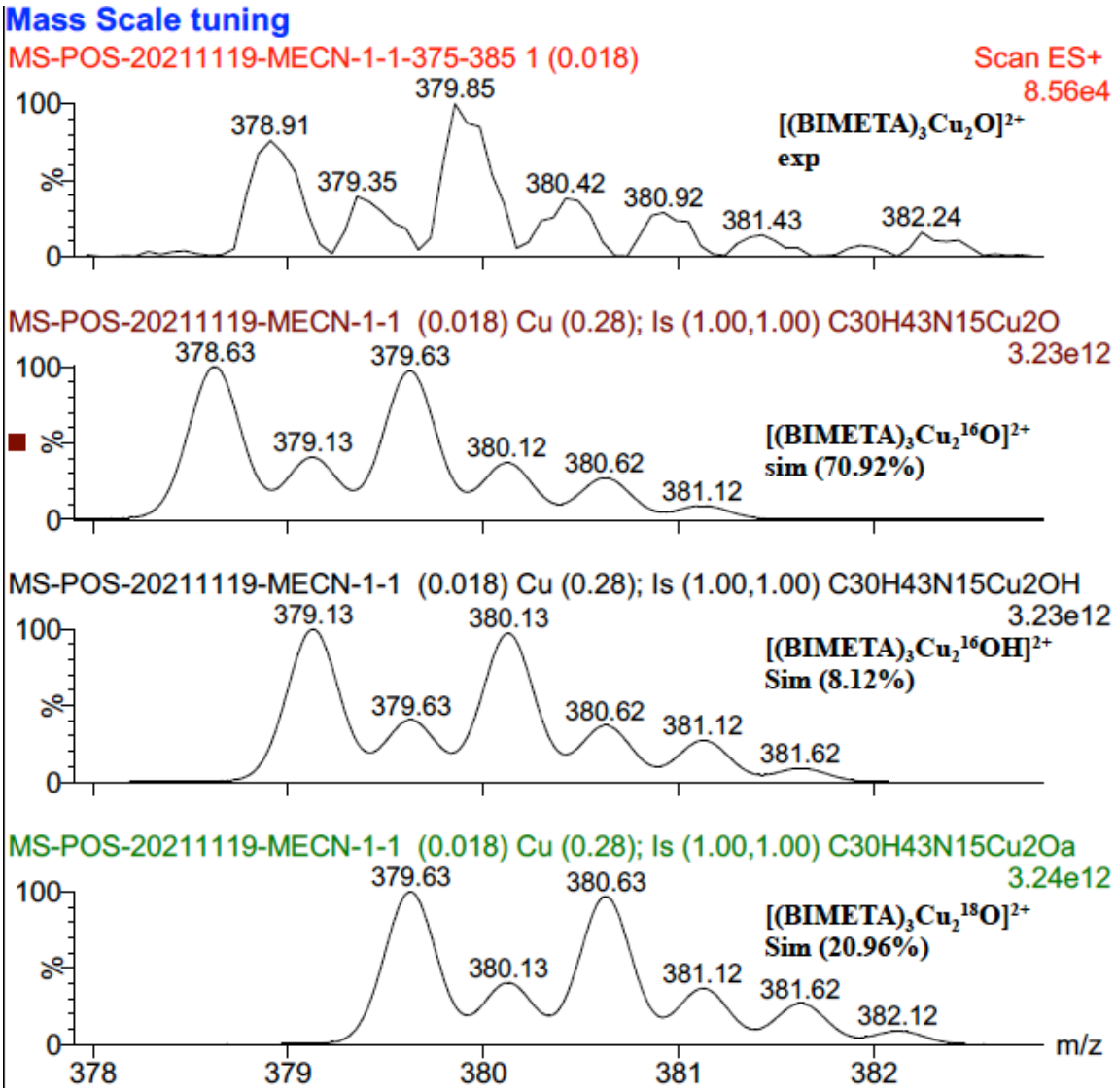

Fig. S9 The full-range ESI mass spectra of (a) $^{16}O_2$-generated **1**^{ox}**;** (b) $^{18}O_2$-generated **1**^{ox}, and the isotope distribution pattern of $^{18}O_2$-generated **1**^{ox}.

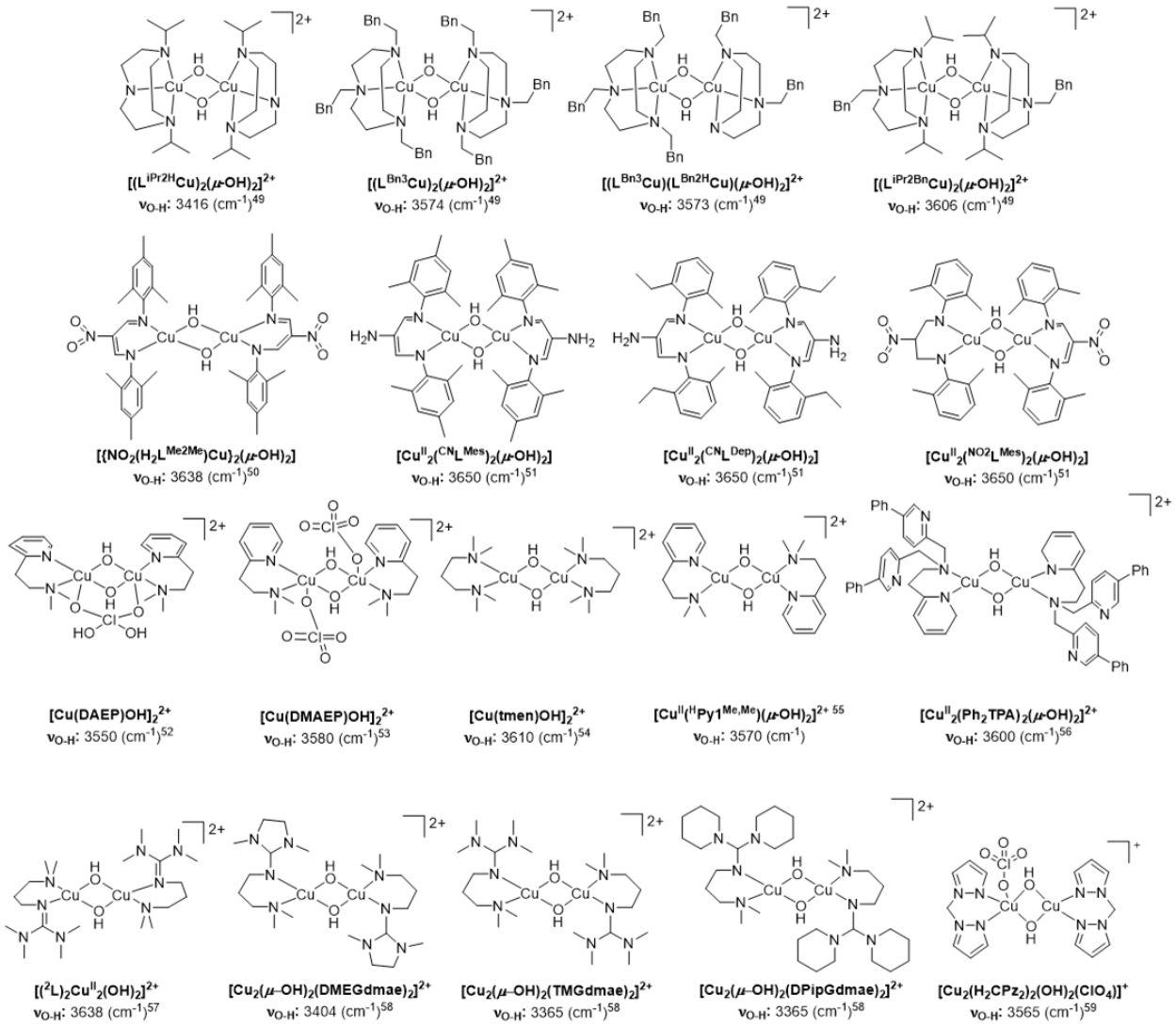

Fig. S10 Typical IR signature and structure of dicopper(II)-bis-μ-hydroxo in relevant papers.

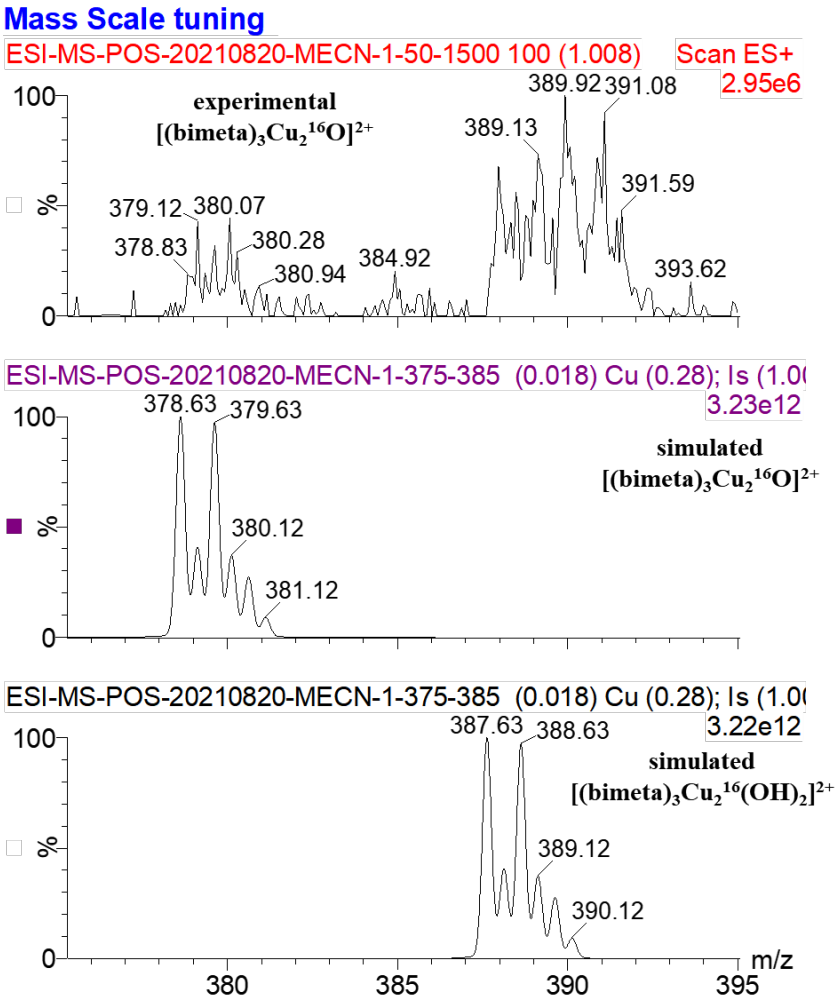

Fig. S11 The isotope distribution pattern of $^{16}O_2$-generated **1**^{ox} measured by ESI-MS and its simulated spectrum including dicopper(II)-bis-μ-hydroxo.

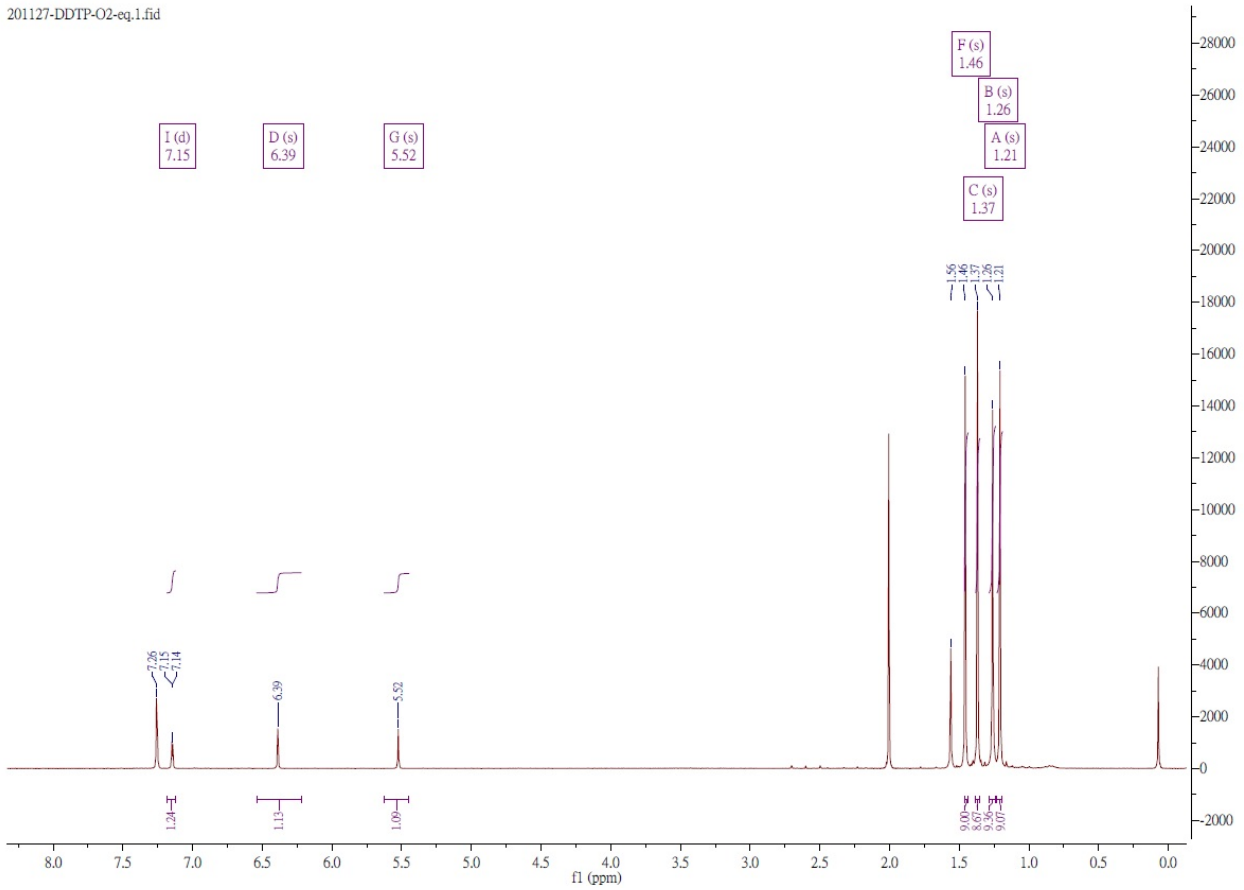

Fig. S12 The ^{1}H NMR spectrum resulting from the stochiometric reaction between TBBP and complex $\mathbf{1^{ox}}$.

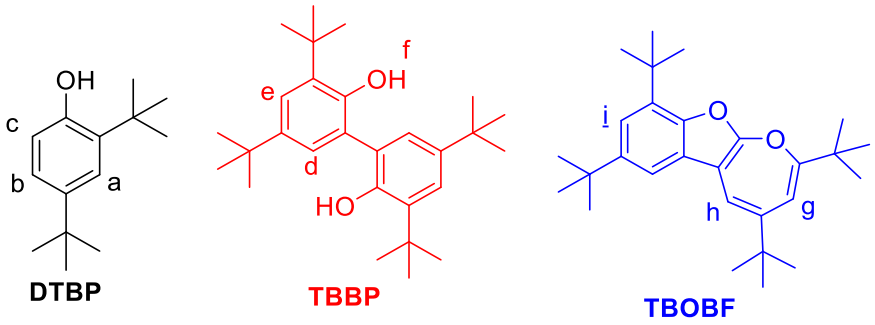

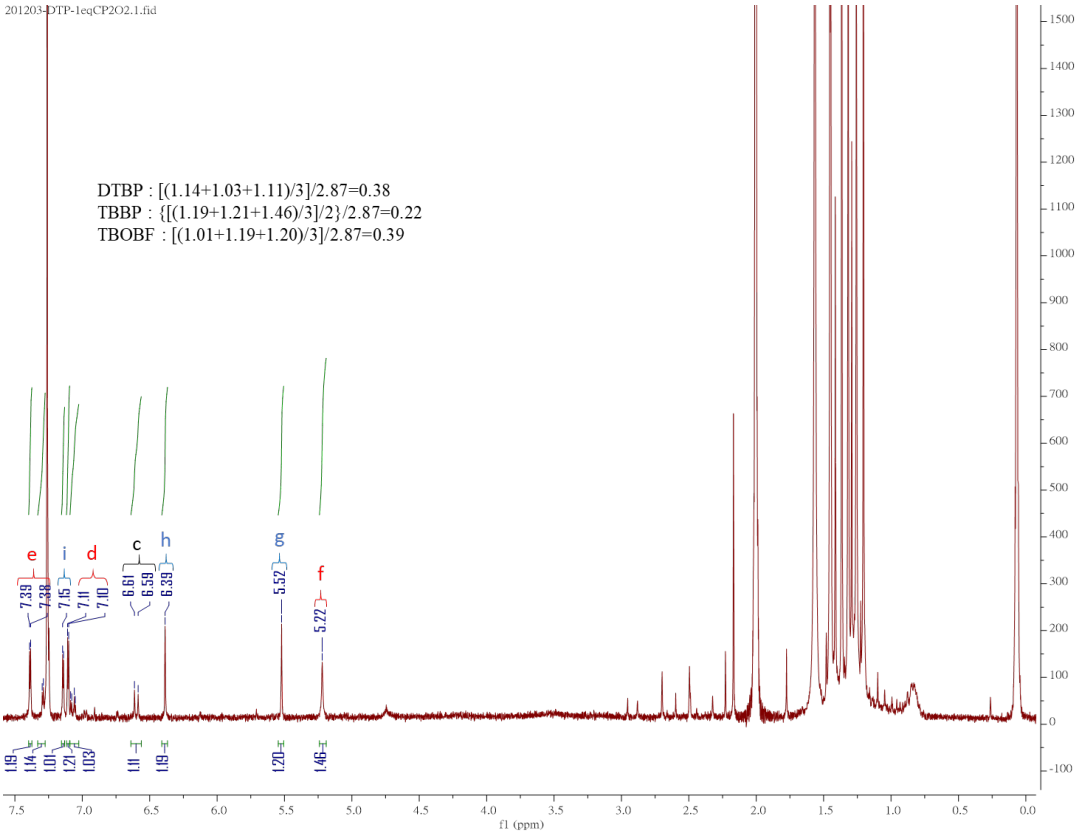

Fig. S13 The ^{1}H NMR spectrum resulting from the stochiometric reaction between DTBP and complex **1^{ox}**

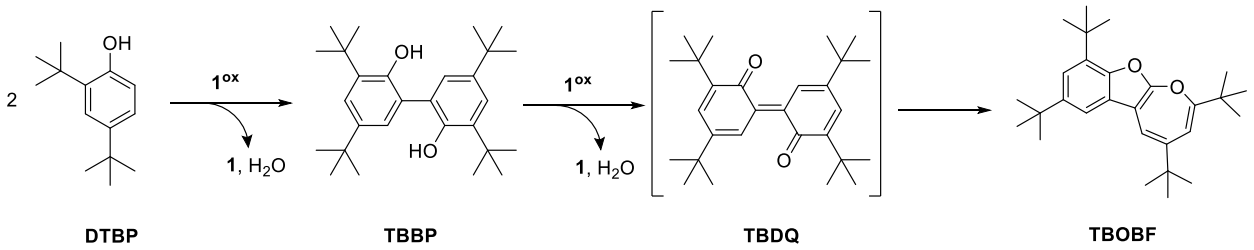

Fig. S14 The proposed mechanism for the formation of TBOBF from the reaction of DTBP and complex $\mathbf{1^{ox}}$

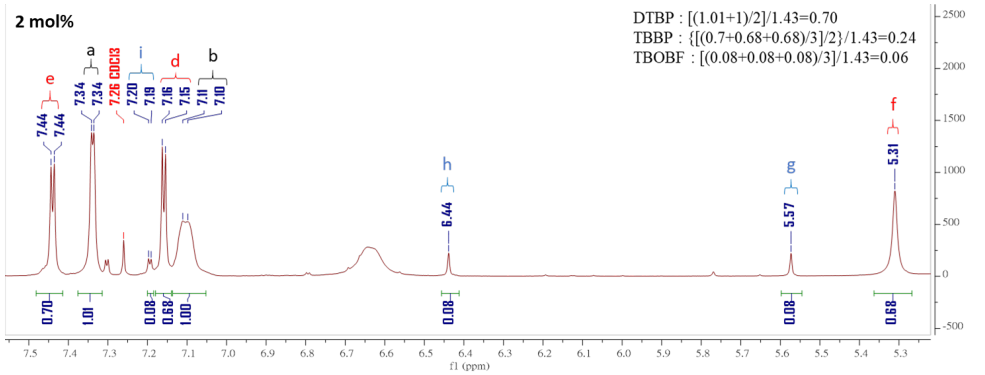
2 mol%
DTBP : [(1.01+1)/2]/1.43=0.70
TBBP : {[(0.7+0.68+0.68)/3]/2}/1.43=0.24
TBOBF : [(0.08+0.08+0.08)/3]/1.43=0.06
f1 (ppm)

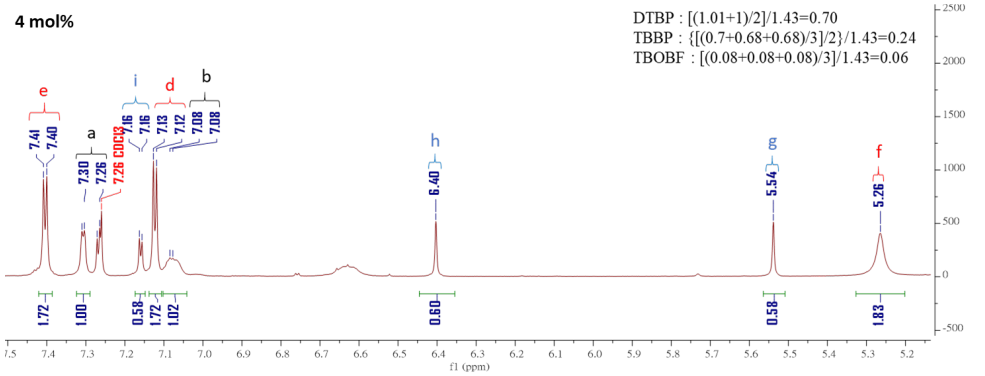
4 mol%
DTBP : [(1.01+1)/2]/1.43=0.70
TBBP : {[(0.7+0.68+0.68)/3]/2}/1.43=0.24
TBOBF : [(0.08+0.08+0.08)/3]/1.43=0.06
f1 (ppm)

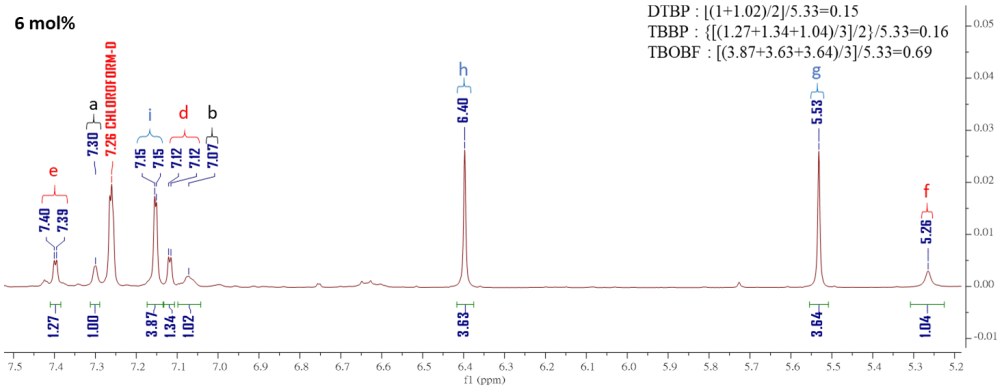
6 mol%
DTBP : [(1+1.02)/2]/5.33=0.15
TBBP : {[(1.27+1.34+1.04)/3]/2}/5.33=0.16
TBOBF : [(3.87+3.63+3.64)/3]/5.33=0.69
f1 (ppm)

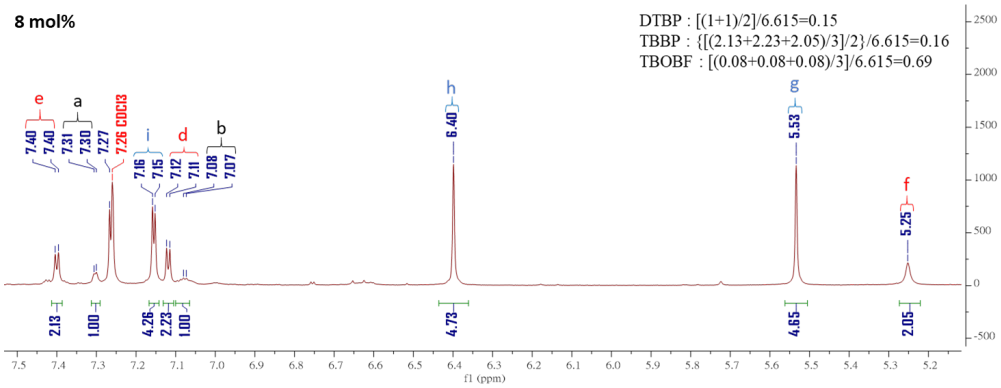
8 mol%
DTBP : [(1+1)/2]/6.615=0.15
TBBP : {[(2.13+2.23+2.05)/3]/2}/6.615=0.16
TBOBF : [(0.08+0.08+0.08)/3]/6.615=0.69
f1 (ppm)

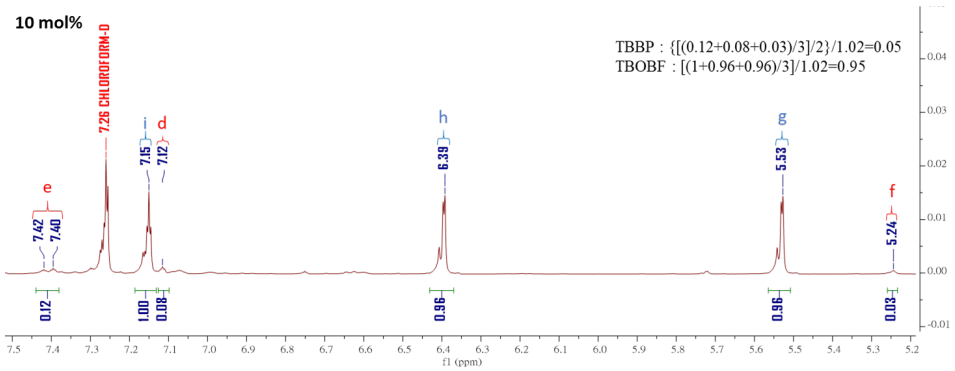

Fig. S15 The ^{1}H NMR spectra of catalytic ytic oxidation of DTBP with different mol% loading of complex $\mathbf{1}^{ox}$ (2 ~ 10 mol%)

10 mol% - 10min

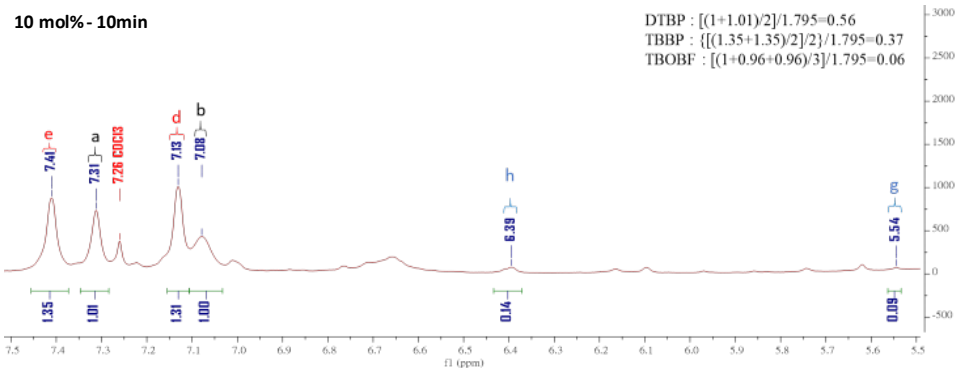

10 mol% - 15min

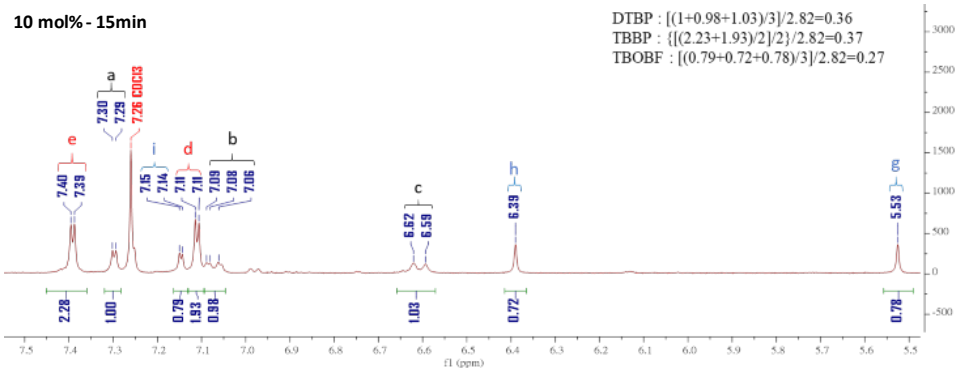

10 mol% - 30min

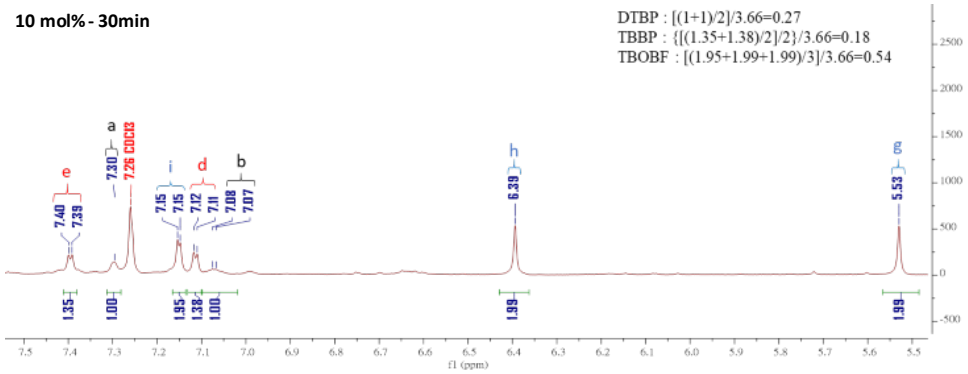

10 mol% - 60min

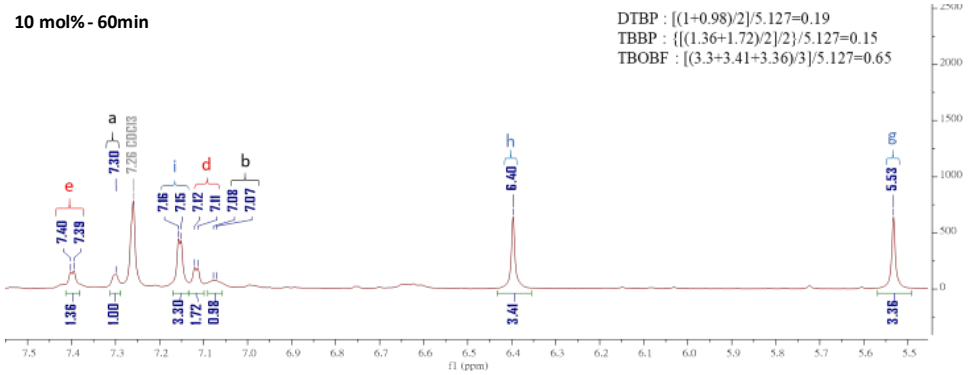

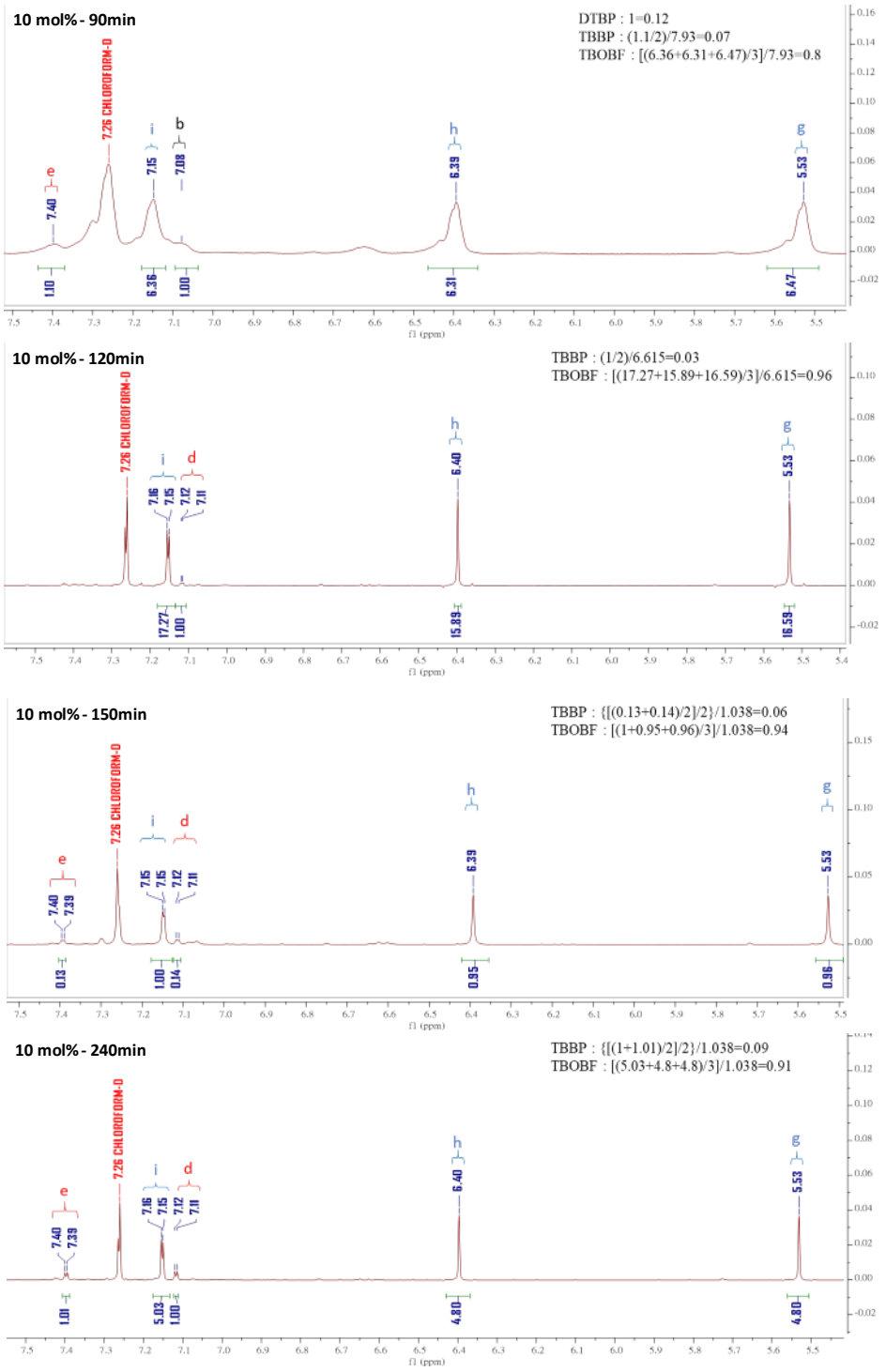

Fig. S16 The ^{1}H NMR spectra of time-course analysis (10 min ~ 240 min) of product distributions (10 mol% loading of catalyst **1**^{ox})

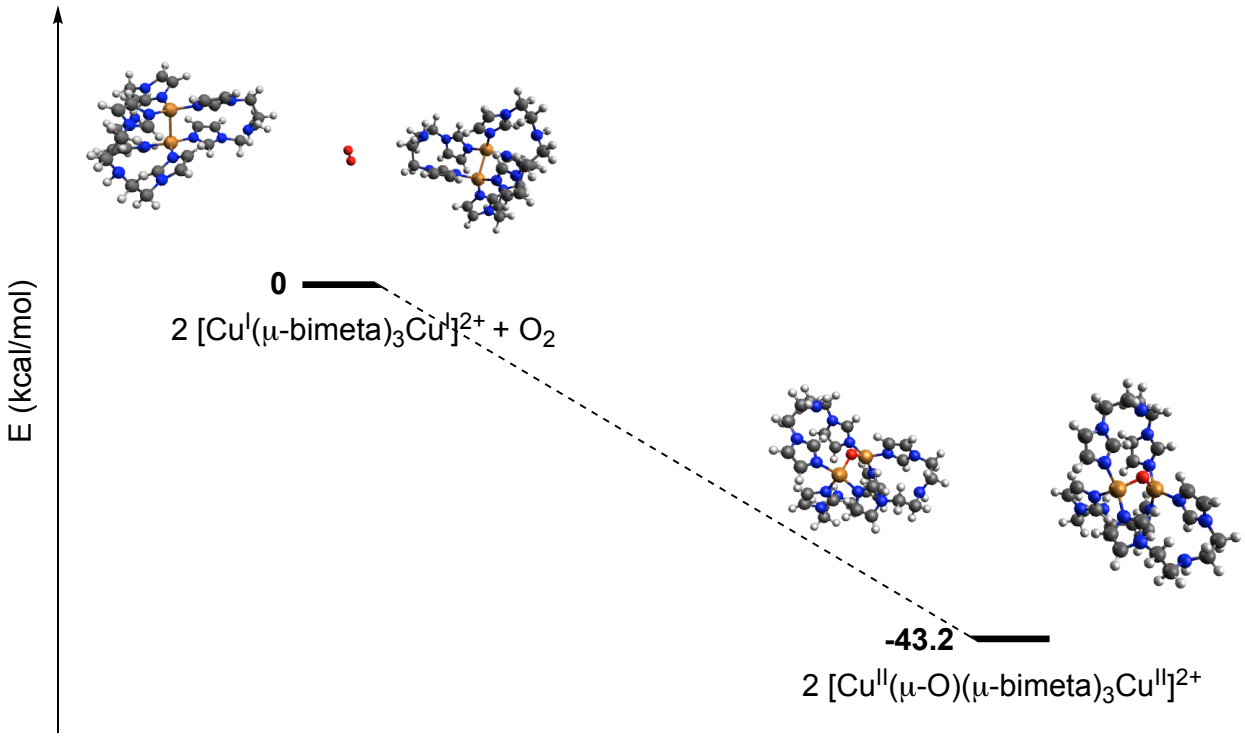

Scheme S1 The energy profile associated with reaction of two equivalents of $[Cu^{I}(\mu\text{-bimeta})_3Cu^{I}]^{2+}$ with O_2 generating the corresponding $2[Cu^{II}(\mu\text{-oxo})(\mu\text{-bimeta})_3Cu^{II}]^{2+}$

Table S1. Selected bond distances (Å) and bond angles (°) of **1** and the corresponding DFT structure

	X-ray structure of complex **1**	DFT structure of complex **1**	DFT structure of complex $\mathbf{1^{ox}}$
Cu(1)−N_{Im}	1.954(5)	2.023	2.069
Cu(2)−N_{Im}	1.970(5)	2.033	2.083
Cu(1)−Cu(2)	3.0521(18)	3.453	3.051
Cu(1)−oxo	n.d.	n.d.	1.835
Cu(2)−oxo	n.d.	n.d.	1.850
∠ Cu(1)-oxo−Cu(2)	n.d.	n.d.	111.8
∠ N_{Im}-Cu(1)−N_{Im}	119.57(4)	119.9	97.0/102.1/117.9
∠ N_{Im}-Cu(2)−N_{Im}	119.926(17)	119.3	97.3/99.2/126.3
Cu(1)−N3 plane	0.13	0.16	0.804
Cu(2)−N3 plane	0.05	0.07	0.725
total angle around Cu(1) center	359	360	317
total angle around Cu(2) center	360	358	323

Table S2. Summary of crystallographic data, intensity collection and structure refinement parameters for complexes **1**

Complex number	1
Empirical formula	$C_{6.58}H_{10}Cu_{0.44}F_{2.67}N_{3.33}P_{0.44}$
Formula weight	228.51
Temperature/K	113(2)
Crystal system	trigonal
Space group	P-3
a/Å	22.8908(4)
b/Å	22.8908(4)
c/Å	13.8848(3)
α/°	90
β/°	90
γ/°	120
Volume/Å^3	6300.7(3)
Z	27
ρ_{calc}g/cm^3	1.626
μ/mm^{-1}	1.187
F(000)	3142.0
Crystal size/mm^3	0.2 × 0.2 × 0.2
Radiation	Mo Kα (λ = 0.71073)
2Θ range for data collection/°	3.582 to 54.088
Index ranges	-29 ≤ h ≤ 28, -18 ≤ k ≤ 27, -17 ≤ l ≤ 16
Reflections collected	41314
Independent reflections	8745 [R_{int} = 0.0313, R_{sigma} = 0.0411]
Data/restraints/parameters	8745/939/646
Goodness-of-fit on F^2	1.026
Final R indexes [I>=2σ (I)][a,b]	R_1 = 0.0874, wR_2 = 0.2170
Final R indexes [all data]	R_1 = 0.1380, wR_2 = 0.2470
Largest diff. peak/hole / e Å^{-3}	0.88/-0.86

[a] $R1 = (\Sigma||F_o|-|F_c||)/(\Sigma|F_o|)$. [b] $wR2 = [\Sigma w(F_o^2-F_c^2)^2/\Sigma w(F_o^2)^2]^{1/2}$

The coordinates of DFT optimized structure (complex **1)**

Cu	-0.00298	-0.00035	-1.69688
Cu	-0.00582	0.00108	1.75626
N	0.92980	-1.79591	-1.75847
N	1.27662	-3.95192	-2.12096
N	-0.64437	-5.68067	-0.61221
N	-0.65249	-4.12932	2.03941
N	-0.65868	-1.91841	1.91708
N	-2.02286	0.09804	-1.76350
N	-4.05874	0.88621	-2.12954
N	-4.59288	3.40918	-0.61039
N	-3.25869	2.62599	2.04453
N	-1.34152	1.52457	1.92465
N	1.09241	1.70147	-1.76895
N	2.79293	3.06908	-2.14030
N	5.24526	2.26537	-0.62477
N	3.89788	1.49946	2.02905
N	1.98329	0.39301	1.91383
C	0.40775	-2.92061	-2.22462
C	2.20052	-2.12222	-1.32390
C	2.42757	-3.45599	-1.53869
C	0.99548	-5.35376	-2.43912
C	0.59484	-6.17603	-1.20708
C	-0.96769	-6.23744	0.70302
C	-0.23683	-5.52049	1.84886
C	-1.77780	-3.69613	2.71463
C	-1.76754	-2.33056	2.63213
C	-0.01628	-3.02739	1.57654
C	-2.72984	1.11723	-2.22862
C	-2.94642	-0.83644	-1.33468
C	-4.21218	-0.35967	-1.55172
C	-5.12700	1.83643	-2.44787
C	-5.64151	2.59024	-1.21432
C	-4.91822	3.96189	0.70612
C	-4.66986	2.96454	1.84840
C	-2.32394	3.37747	2.73110
C	-1.14680	2.68508	2.64998
C	-2.62118	1.52694	1.57667
C	2.32859	1.80226	-2.23418
C	0.74479	2.97026	-1.34543
C	1.79059	3.82723	-1.56569
C	4.15020	3.51737	-2.45992
C	5.06175	3.58380	-1.22735
C	5.88559	2.26884	0.69223
C	4.89707	2.55216	1.83402
C	4.08385	0.30981	2.70727
C	2.89429	-0.36139	2.62917
C	2.62446	1.50139	1.56894
H	-1.42165	-5.84857	-1.24901
H	-0.58188	-3.02790	-2.64400
H	2.85614	-1.38047	-0.89196
H	3.29122	-4.07979	-1.36207
H	0.19778	-5.36545	-3.18834

H	1.88532	-5.78615	-2.90558
H	1.39436	-6.10599	-0.46075
H	0.53839	-7.23569	-1.50933
H	-2.04709	-6.13900	0.85599
H	-0.72973	-7.31184	0.78077
H	0.84407	-5.51647	1.68344
H	-0.41524	-6.05618	2.78611
H	-2.45261	-4.38505	3.20024
H	-2.46399	-1.62037	3.05259
H	0.89659	-3.07299	1.00002
H	-4.34444	4.16880	-1.24216
H	-2.32247	2.02726	-2.64415
H	-2.63767	-1.77818	-0.90525
H	-5.18671	-0.79193	-1.37953
H	-4.73202	2.53525	-3.19181
H	-5.94642	1.28763	-2.92085
H	-5.98640	1.86022	-0.47323
H	-6.52764	3.17353	-1.51757
H	-4.29242	4.84559	0.86625
H	-5.96739	4.29458	0.78060
H	-5.20729	2.02800	1.67576
H	-5.04865	3.38288	2.78579
H	-2.58485	4.30284	3.22244
H	-0.18564	2.92882	3.07771
H	-3.11480	0.76462	0.99099
H	5.77896	1.67076	-1.25681
H	2.91323	0.99273	-2.64600
H	-0.22547	3.17558	-0.91756
H	1.90353	4.88801	-1.39772
H	4.55613	2.82589	-3.20482
H	4.08540	4.50183	-2.93213
H	4.60386	4.24763	-0.48523
H	6.01039	4.05828	-1.53124
H	6.33712	1.28451	0.85163
H	6.69890	3.01029	0.76818
H	4.35495	3.48595	1.66125
H	5.44826	2.67066	2.77179
H	5.01824	0.06894	3.19174
H	2.62598	-1.31772	3.05301
H	2.20818	2.31424	0.99120

The coordinates of DFT optimized structure (complex **1^{ox})**

Cu	0.14112	0.80015	1.20104
Cu	-0.04766	-0.61338	-1.74015
N	-0.27146	-0.68309	2.61003
N	-0.36695	-2.61194	3.68894
N	0.29595	-5.14145	1.92928
N	-0.54912	-4.68617	-0.96443
N	-0.09867	-2.68401	-1.78253
N	1.91433	1.57245	1.81461
N	3.73718	2.81163	1.69881
N	4.88998	2.82400	-1.14419
N	4.03750	0.11129	-2.43209
N	1.88049	-0.35154	-2.38381
N	-1.41368	2.26099	1.84966
N	-3.31441	3.38586	1.68314
N	-5.19080	2.22692	-0.57498
N	-3.67712	0.99537	-2.98257
N	-1.92810	-0.25275	-2.49157
C	0.18060	-1.92957	2.65193
C	-1.14837	-0.55390	3.66785
C	-1.21558	-1.73891	4.34580
C	-0.09169	-3.99555	4.09694
C	-0.56842	-5.06578	3.10989
C	-0.07298	-6.19073	0.97413
C	-1.08861	-5.72055	-0.07867
C	0.40984	-4.86004	-1.94492
C	0.68059	-3.61373	-2.43991
C	-0.82118	-3.36535	-0.90302
C	2.57388	2.47297	1.09780
C	2.68627	1.32002	2.93019
C	3.82159	2.08086	2.87073
C	4.75758	3.71921	1.16515
C	5.63871	3.07405	0.08857
C	5.61823	2.04120	-2.14733
C	5.37560	0.53031	-2.00128
C	3.67274	-0.22890	-3.72122
C	2.33581	-0.51389	-3.67758
C	2.92556	0.03054	-1.66560
C	-2.61099	2.29182	1.28758
C	-1.33959	3.37926	2.65203
C	-2.50864	4.08576	2.56369
C	-4.70071	3.73547	1.34714
C	-5.05794	3.62098	-0.13720
C	-5.69409	2.06895	-1.94239
C	-4.58961	2.14113	-3.00820
C	-3.89462	-0.24402	-3.55985
C	-2.80160	-1.00585	-3.24949
C	-2.48603	0.94207	-2.34995
H	1.25646	-5.29813	2.23217
H	0.87547	-2.38014	1.95912
H	-1.65713	0.37759	3.86204
H	-1.76852	-2.03775	5.22353
H	0.98423	-4.09960	4.28058
H	-0.59369	-4.14134	5.05589

H	-1.59234	-4.83484	2.79322
H	-0.60995	-6.02456	3.65561
H	0.83600	-6.52051	0.46102
H	-0.49737	-7.07870	1.47162
H	-1.98514	-5.30860	0.39256
H	-1.40278	-6.57066	-0.69217
H	0.79026	-5.83589	-2.20674
H	1.37216	-3.32576	-3.21717
H	-1.53905	-2.94117	-0.21573
H	4.59861	3.71124	-1.55152
H	2.24837	2.88285	0.15403
H	2.36585	0.62805	3.69430
H	4.65814	2.18272	3.54558
H	4.25246	4.60659	0.76948
H	5.37519	4.04631	2.00515
H	6.02065	2.11890	0.46780
H	6.51377	3.72676	-0.07109
H	5.29009	2.35620	-3.14284
H	6.70569	2.21418	-2.10041
H	5.50523	0.21424	-0.96242
H	6.10038	-0.02402	-2.60431
H	4.38598	-0.24349	-4.53159
H	1.67846	-0.81297	-4.48093
H	2.91191	0.25972	-0.61123
H	-5.81584	1.73625	0.06356
H	-3.00689	1.57315	0.58622
H	-0.45607	3.60370	3.23216
H	-2.83884	5.00139	3.03098
H	-5.38203	3.11872	1.94774
H	-4.84446	4.77153	1.66261
H	-4.28231	4.11535	-0.73403
H	-5.99225	4.18888	-0.29130
H	-6.18775	1.09441	-2.01402
H	-6.44910	2.83235	-2.19745
H	-3.98451	3.04380	-2.88802
H	-5.04340	2.18513	-4.00265
H	-4.77965	-0.45644	-4.14066
H	-2.57972	-2.02532	-3.52749
H	-2.04163	1.75755	-1.79965
O	-0.20492	0.83826	-0.58678